Hindawi
Advances in Civil Engineering
Volume 2022, Article ID 4121193, 14 pages
https://doi.org/10.1155/2022/4121193

Research Article

Stability Prediction of Residual Soil and Rock Slope Using Artificial Neural Network

Mahesh Paliwal,[1] Himkar Goswami,[2] Arunava Ray,[1] Ashutosh Kumar Bharati,[1] Rajesh Rai,[1] and Manoj Khandelwal[3]

[1]*Department of Mining Engineering, Indian Institute of Technology (BHU) Varanasi, Varanasi, India*
[2]*School of Computer Science and Eng., Vellore Institute of Technology, Vellore, Tamil Nadu, India*
[3]*Institute of Innovation, Science and Sustainability, Federation University Australia, Ballarat 3350, VIC, Australia*

Correspondence should be addressed to Manoj Khandelwal; m.khandelwal@federation.edu.au

Received 27 October 2021; Revised 15 March 2022; Accepted 7 April 2022; Published 30 April 2022

Academic Editor: Hadi Hasanzadehshooiili

Copyright © 2022 Mahesh Paliwal et al. This is an open access article distributed under the Creative Commons Attribution License, which permits unrestricted use, distribution, and reproduction in any medium, provided the original work is properly cited.

A sudden downward movement of the geomaterial, either composed of soil, rock, or a mixture of both, along the mountain slopes due to various natural or anthropogenic factors is known as a landslide. The Himalayan Mountain slopes are either made up of residual soil or rocks. Residual soil is formed from weathering of the bedrock and mainly occurs in gentle-to-moderate slope inclinations. In contrast, steep slopes are mostly devoid of soil cover and are primarily rocky. A stability prediction system that can analyse the slope under both the condition of the soil or rock surface is missing. In this study, artificial neural network technology has been utilised to predict the stability of jointed rock and residual soil slope of the Himalayan region. The database for the artificial neural network was obtained from numerical simulation of several residual soils and rock slope models. Nonlinear equations have been formulated by coding the artificial neural network algorithm. An android application has also been developed to predict the stability of residual soil and rock slope instantly. It was observed that the developed android app provides promising results in predicting the factor of safety and stability state of the slopes.

1. Introduction

Landslide is defined as the downslope movement of a large mass of rocks, rubbles, soil, or a mixture of all, owing to various natural and anthropogenic factors. This downslope movement of soil and rock through the influence of gravity leads to a kind of "mass wasting" [1]. Landslide consists of five various types of slope movement: falls, topples, slides, spreads, and flows [2]. These types are segmented based on their geological make (bedrock, debris, or Earth). Some of the common landslide types are debris flows and rockfalls. Nearly every single landslide has numerous reasons for its occurrence [3, 4]. Slope movement occurs once forces operating down the slope under the influence of gravity surpass the strength of the ground materials that hold the slope [5]. Some of the major factors increasing the landslide occurrence are the impact of downslope forces and the reduced strength of the bedrock or the soil constituting the slope. Landslides are set off on the slopes, which are already on the rim of movement by rainfall, snowmelt, changes in water level, stream erosion, changes in groundwater, earthquakes, volcanic activity, disruption by human activities, or any permutation of these factors [6].

Landslides mostly result in property damage, injuries, and many fatalities [7]. It also negatively alters a variety of natural resources. Water bodies, fisheries, sewage disposal systems, forests, dams, and roadways the whole lot have an effect for a long time after a landslide occurrence [8]. These adverse economic effects of landslides incorporate the expenses for the restoration of structures, loss of property, interruption of transportation routes, and medical expenses in the instance of injuries, and unforeseen costs in the form of lost goods, freshwater accessibility, level, and condition are also impacted [9]. People might decrease their risks of

landslides by studying probable landslide hazards and undertaking measures to mitigate those hazards. Due to the isolated nature of the landslide event, they usually occur in an instance without any public forewarning.

Landslide risk mitigation is generally categorised into direct and indirect methods [10]. The direct method includes geometric methods, where the geometry of the hillside is altered (in general the slope); hydrogeological methods, where an attempt is made to decrease the groundwater level or to reduce the water content of the slope material; chemical and mechanical methods, where efforts are made to build up the shear strength of the unsteady mass or else to establish dynamic external forces or passive to counter the destabilising forces. These methods adjust to a certain extent with the kind of material that makes up the mountain slope [11–13]. The indirect method of landslide risk mitigation includes landslide hazard zonation maps, landslide hazard charts, and early warning techniques, which is generally used to avoid vulnerable areas for developmental works [14–17].

The Himalayan Mountain slopes are either made up of residual soil or rocks. Residual soil is formed from weathering of the bedrock and mostly occurs in gentle-to-moderate slope inclinations (<50°–60° slope angle). In contrast, steep slopes (>60° slope angle) are mostly devoid of soil cover and are primarily rocky [1]. Many times, there is a sudden change in the slope geomaterial (soil or rock) within a few hundred meters of distance. The stability analyses of both cases of slope material are different from each other and cannot be used uniformly. A stability prediction system that can analyse the slope under both the condition of the soil or rock surface is missing.

A detailed study of the residual soil and rock slopes of the Himalayan region was carried out by Ray et al. [18] and Ray et al. [19], respectively. In the present study, the artificial neural network analysis was used for stability prediction of residual soil and rock slope using the numerical simulation data of Ray et al. [18] and Ray et al. [19]. Nonlinear equations have been formulated by coding the artificial neural network algorithm. An android application has also been developed to predict the stability of residual soil and rock slope instantly. The mobile application was rendered user friendly with a basic GUI and is available for public use to quickly identify the stability state of the residual soil and rock slope of the Himalayan region.

2. Area of Study

The study area is located in the Himalayan region in the Indian states of Uttarakhand and Himachal Pradesh, which lies at the convergence zone of two lithospheric plates. One is the Indian plate in the south, and the other is the Eurasian plate in the north. The prevalence of a large number of discontinuities makes this region geologically very fragile and susceptible to frequent landslides. A slight imbalance in elements of shear stress and strength factors might trigger landslides. The Himalayan Mountain slopes can be classified into two distinct categories based on stratigraphy, namely, rock slopes and soil slopes. The rock slopes have highly fractured rock mass at the surface and are devoid of any soil cover. The failure in rock slopes is governed mainly by the discontinuities present within the rock mass. The soil slopes, on the other hand, are formed from the weathering of bedrock and are also referred to as residual soil slope. Slope failure in residual soil slope is a complex phenomenon involving various factors such as slope topography, depth of soil cover, the grain size distribution of the soil, inherent heterogeneity in the geomechanical properties of the soil, and the presence of water. Ray et al. [1] have carried out extensive literature studies of the Himalayan region and concluded that up to moderate slope (<50°–60°), the thickness of residual soil varies from 2 to 10 m, with some places exceeding 10 m before encountering the weathered bedrock. Previous studies concerning slope stability were limited either to residual soil slopes or rock slopes. The current study focuses on the slope stability problem associated with jointed rock slopes and residual soil slopes in the Himalayan Range.

A database of 400 slope models, which were previously analysed by Ray et al. [18] using a numerical simulation technique, has been used for the stability analysis of the residual soil slope. Thirteen major influencing parameters have been considered during numerical simulation, which include Young's modulus of residual soil (Es), unit weight of soil (γ_s), shear strength parameter of residual soil (cohesion (Cs) and angle of internal friction (Φs)), Young's modulus of the weathered rock mass (Er), shear strength parameter of the weathered rock mass (cohesion (Cr) and angle of internal friction (Φr)), unit weight of weathered rock (γ_r), strength parameter of the soil-rock joint interface (cohesion (Cj) and angle of internal friction (Φj)), average slope angle (α), slope height (H), and residual soil depth (D). The obtained results indicate that all the parameters are affecting the FOS of the residual soil slopes. However, the impact of all those thirteen parameters was not uniform as can be seen from correlation analysis (Table 1). For developing the ANN models, all those parameters whose correlation coefficient is more than 0.2 are considered.

Similarly, a database of 1200 slope models, which were previously analysed by Ray et al. [19], using a numerical simulation technique, has been used for the stability analysis of the rock slope. Thirteen major influencing parameters have been considered during numerical simulation, which include Young's modulus of the weathered rock mass (Er), the tensile strength of the weathered rock mass (Tr), Poisson's ratio of weathered rock mass, unit weight of weathered rock mass (γ_r), shear strength parameter of the weathered rock mass (cohesion (Cr) and angle of internal friction (Φr)), shear strength parameter of the bedrock (cohesion (Cbr) and angle of internal friction (Φbr)), slope angle (α), slope height (H), width of weathered layer (D), main joint orientation ($Dip1$), and cross joint orientation ($Dip2$). The obtained results indicate that all the input parameters affect the FOS of the rock slopes. However, the impact of all those thirteen parameters was not uniform as can be seen from correlation analysis (Table 2). For developing the ANN models, all those parameters whose correlation coefficient is more than 0.2 are considered.

Table 1: Correlation analysis of input parameters of the residual soil slope with the FOS.

Number	Parameters	Correlation coefficient for FOS
1	Slope angle (deg)	−0.73
2	Slope height (m)	−0.32
3	Soil depth (m)	−0.43
4	Soil friction angle (deg)	0.30
5	Soil cohesion (kPa)	0.21
6	Soil unit weight (kN/m^3)	0.16
7	Soil Young's modulus (kPa)	0.27
8	Weathered rock friction angle (deg)	−0.04
9	Weathered rock cohesion (kPa)	−0.03
10	Weathered rock unit weight (kN/m^3)	−0.03
11	Weathered rock Young's modulus (MPa)	−0.06
12	Soil-rock interface cohesion (kPa)	0.06
13	Soil-rock interface friction angle (deg)	0.12

Table 2: Correlation analysis of input parameters of the rock slope with the FOS.

Number	Parameters	Correlation coefficient for FOS
1	Slope angle (deg)	−0.73
2	Slope height (m)	−0.32
3	Weathered layer thickness (m)	−0.43
4	Major joint orientation (deg)	0.30
5	Cross joint orientation (deg)	0.21
6	Weathered rock friction angle (deg)	−0.14
7	Weathered rock cohesion (kPa)	−0.08
8	Weathered rock unit weight (kN/m^3)	−0.13
9	Weathered rock Young's modulus (MPa)	−0.11
10	Weathered rock Poisson's ratio	−0.05
11	Weathered rock tensile strength (kPa)	−0.03
12	Bedrock cohesion (kPa)	0.06
13	Bedrock friction angle (deg)	0.12

3. Methodology

Four hundred numerical simulation models were analysed by Ray et al. [18] using various permutation combinations of the height of the slope, the angle of the slope, and the thickness of the layer of residual soil. The height of the slope varied from 50 m to 500 m, with an interval of 50 m. The overall slope angle varied from 15° to 60°, with an interval of 15°. The thickness of the layer of the residual soil varied from 0.5 m to 15 m (0.5 m, 1 m, 2 m, 3 m, 4 m, 5 m, 7 m, 9 m, 12 m, and 15 m). Thus, the height of the slope resulted in ten variations, the thickness of residual soil resulted in ten variations, and the angle of slope caused four variations, leading to 400 models (i.e., $10 * 10 * 4 = 400$). About 1200 numerical simulation models were analysed by Ray et al. [19] using various permutation combinations of slope height, slope angle, weathered layer thickness, and variations of each cross joint set (models were prepared with two joint sets). There were five variations in slope height, three variations in slope angle, five variations in weathered layer thickness, and four variations of each cross joint set. Using the numerical simulation data obtained from analysing the residual soil slopes and the rock slopes, ANN models were prepared to predict the FOS of the investigated slopes.

3.1. Artificial Neural Network Model. The natural nervous system, such as the brain processing information, is the main inspiration behind the information processing paradigm of an ANN (artificial neural network). It comprises many highly interconnected processing elements (neurons) functioning in concurrence to resolve a particular problem [20]. The artificial neural network is a framework instead of an algorithm for various distinct machine learning algorithms, through which they might work together and process complex computations [21]. These types of systems tend to "learn" in order to implement tasks by ruminating the examples, mostly lacking the need of being programmed with any task-specific instructions. An ANN primarily moves through a training phase, where it figures out how it might perceive the patterns in data, whether using visual, audio, or literal aid [22]. The disparity between the two outputs will be corrected by utilising backpropagation [23]. This further implies that the network will work in reverse, going from the output nodes to the input nodes in order to alter the weight of the connections amongst the nodes up until the variation between the actual and desired outcome yields the minimal conceivable error. Throughout the training and testing phases, the ANN is trained on what things to search for and what its output ought to look like, utilising binary yes/no query types [24].

The activation function is imperious for an ANN to learn and build the logic of some genuinely complex problem. The crucial notion here is to convert an input signal of a node in an ANN into an output signal of the node. The output signals might be utilised as an input to the next layer in the neural network stack. The activation function decides if a neuron ought to be activated by assessing the weighted sum and then further adding up the bias [25]. This is done to get non-linearity into the output of a node. If there is no activation function, then the output signal will be a more straightforward linear function, which is limited in its complexity and has much less learning power [26]. Deficient in a proper activation function, the model will not learn complex data such as images, videos, audio, and speech. Nonlinear functions have a higher degree, that is, more than one, and they follow a polynomial curve. Some essential types of activation functions are threshold activation function, binary step function, sigmoid activation function, hyperbolic tangent function, and rectified linear units [27].

3.2. Network Architecture. The neural network is generally formulated into various layers. In Figure 1, the input layer is represented in yellow. It directly takes the input from the external source. Each of the nodes in the input layer is then interconnected with the nodes of the next layer. Blue and green colours denote the hidden layers. Hidden layers are interconnected networks of nodes that exist between the output and the input nodes. Hidden layers remain hidden from the outside world and are responsible for the computation done by the neural network. Edges are formed by the connection of nodes between two different layers, and each edge is allotted some weight based on the relative significance of the connection between the nodes. All the node values are based on the inputs provided by the user. These are then multiplied with the assigned weight of their edges, and then it is all summed up to get the value of the particular, mostly done for the hidden layers [21, 28]. Based on this summed-up value, nodes of the hidden layer will be "activated" or not, which is decided by predefined activation functions. Thus, the hidden layers take the input from the input layer and compute based on the weights and the activation function. Then, that result is propagated to the next layer of nodes until it reaches the final output node, where one can view the outcome [28]. Various performance indices such as the coefficient of determination (R^2), residual error, root mean square error (RMSE), the variance accounted for (VAF), and the learning rate are used for assessing the efficacy of the developed ANN models [21, 23, 27, 29, 30].

3.3. Mobile Application. Developing a mobile application means developing a software application for smartphones, tablets, and other handheld devices. This application can be preinstalled in mobiles or supplied on a server or client-side as web applications to give a "mobile application-like" familiarity in a web browser portal. This is possible with an application-like processing experience. Mobile application developers consider a long arrangement of screen sizes, hardware specifications, and configurations before

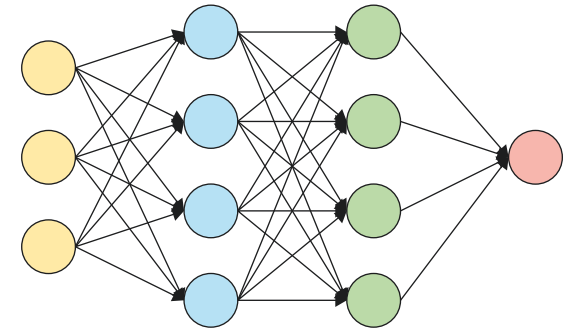

Figure 1: Network architecture.

proceeding with the development process. The mobile application developers should also consider the extensive diversity of screen sizes, hardware specs, and settings due to fierce competitiveness in mobile applications and changes across all platforms. Being a part of the mobile app development process, mobile user interface (UI) designing will be a vital step in the making of mobile apps. The mobile app UI design's objective is primarily to make the experience of the interface more comprehensible. Much more functionalities will be followed by inculcating mobile enterprise application platforms or integrated development environments (IDEs).

Utilising an artificial neural network (ANN) technique, a microstrip patch antenna will be constructed. In order to design a proper mobile application, both the investigation and creation problems for constructing microstrip patch antennas are taken into. An analysis problem denotes the estimate of resonant frequency, while a synthesis problem denotes the estimate of dimensions. Both these are reciprocal of each other. The outcomes are put into operation utilising a mobile application. Back-propagation of the artificial neural networks is mainly utilised for training the neural network in order to minimise the error and computation time. So, the geometric dimensions of the micro antenna patch will be obtained with higher accuracy in lesser computation time in comparison to the simulation software. Sometimes, the size of the antenna might be a limitation, especially in mobile and wireless applications.

The work required dealing with low-level graphics, high accuracy prediction using ANN, and the vast portion of the app, React Native and Flutter, did not fit the use case, and it is just too much overhead to build the app with *C++*. Thus, the viable option is to create separate apps for each platform or use Kotlin Multiplatform to share most code. In order to create separate apps, an Android app will be created using Kotlin, and then the code will be shared with iOS, too (Figure 2). It has low risk and high returns. Therefore, Kotlin Multiplatform (KMP) is the obvious choice. The KMP-based app can scale well and would be beneficial in the long run, even if some problems with tooling and language might occur. Kotlin Multiplatform is created by Jetbrains and uses Kotlin as the programming language. It is more a set of technologies than a framework. It provides common business logic, high performance, compiles to bytecode for

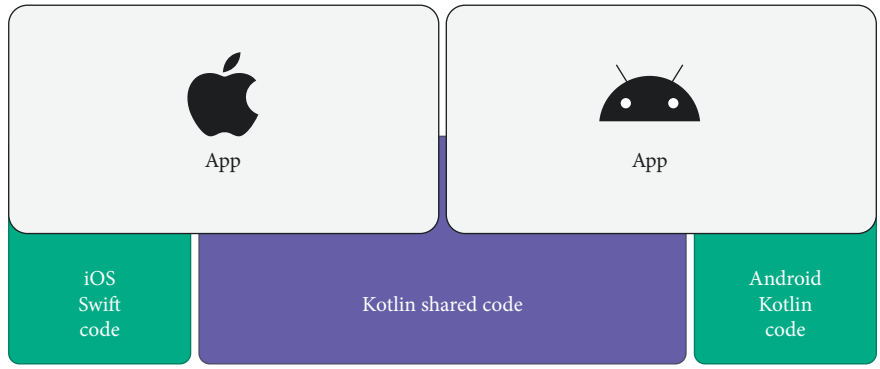

Figure 2: KMP architecture.

Android and native for iOS, good interop with Java, and very little to no change for Android developers.

Kotlin Multiplatform Mobile or KMM is a subset of KMP focusing on making the tech stable or used on mobile platforms, namely, Android and iOS and provides improved and better tooling for this use case. Kotlin Multiplatform provides an advantage over other platforms in making scalable and maintainable apps using a single codebase. Although the code-sharing is slightly less than that with other cross-platform solutions, UI cannot be shared; this gives the advantage of creating a user experience that aligns with the platform's guidelines and best practices. KMP can target JVM for a faster iteration cycle as the whole code can be run and tested on the PC rather than a mobile device. It also provides the future possibility of using the same code for other platforms such as Web and Desktop with minimal changes.

4. Prediction of Stability Class and Factor of Safety

The sample dataset comprises information to build the predictive model. The inputs are independent variables, the targets are the dependent variables, and the unused variables will not be used as inputs or targets. Furthermore, some instances might be training instances that are utilised to create the model, selection instances are utilised for picking the optimum order, testing instances are utilised to validate the model's working, and unused instances are not contemplated at all.

4.1. Prediction of Stability Class or Risk Factor for Residual Soil Slope. The total number of instances is 400. The number of training instances is 240 (60%), the number of selection instances is 80 (20%), the number of testing instances is 80 (20%), and the number of unused instances is 0 (0%). Table 3 lists the number of variables and their type. Table 4 lists the minimum, maximum, mean, and standard deviation for all of the variables in the dataset. In this model, the FOS is the output. As a consequence, no mean and standard deviation are shown for them. The minimum column shows the class of the nominal variable with the least number of appearances. In contrast, the maximum column shows the class of the nominal variable with a significant number of impressions.

Table 3: Variable table for residual soil.

Sr. no.	Name	Use
1	Slope angle (deg)	Input
2	Slope height (m)	Input
3	Soil cohesion (kPa)	Input
4	Soil friction angle (deg)	Input
5	Young's modulus of soil (MPa)	Input
6	Soil depth (m)	Input
7	FOS class one	Target
8	FOS class two	Target
9	FOS class three	Target
10	FOS class four	Target

Slope angle, slope height, soil cohesion, soil friction angle, Young's modulus of soil, and soil depth are used as inputs in the artificial neural network. FOS class four, FOS class three, FOS class two, and FOS class one are used as target outputs. The output class is defined based on the FOS range/class for a particular slope profile. This range/class is listed in Table 5.

The most suitable neural network architecture was deduced by training, testing, and validating different combinations of hidden layers and associated neurons. A single hidden layer having a range of 2–15 neurons has been opted to train the neural network model. The number of neurons in the rest two layers, that is, the input layer and output layer, are constrained to the number of input variables and output variables, respectively [31]. The normalising of the input data was performed and the training process is initiated by randomly varying the number of neurons and their associated weights. The network with 6-3-4 architecture (six neurons in the input layer, three neurons in a single hidden layer, and four neurons in the output layer) is selected based on maximum training performance and minimum training error for the developed ANN model after simulation of various network combinations (Table 6). The selected ANN model has a learning rate and momentum of 0.91 and 0.014, respectively, and its architecture is shown in Figure 3.

4.2. Prediction of Factor of Safety for Jointed Rock Slope. The data set includes valuable information for constructing a predictive model. There is a data matrix where columns

Table 4: Data statistics used for prediction.

Sr. no.	Parameters of slope	Minimum	Maximum	Mean	Standard deviation
1	Slope angle (deg)	15	60	37.5	16.791
2	Slope height (m)	50	500	275	143.794
3	Soil cohesion (kPa)	18	20	18.99	0.5730
4	Soil friction angle (deg)	13.05	50.84	32.15	11.0671
5	Young's modulus of soil (MPa)	17.06	122.55	68.87	29.5496
6	Soil depth (m)	0.5	15	5.85	4.61038
7	FOS	—	—	—	—

Table 5: Classification of FOS for residual soil slope in four classes.

FOS range	Risk	Class
<1	High risk	FOS class one
1–1.5	Medium risk	FOS class two
1.5–2	Low risk	FOS class three
>2	Very low risk	FOS class four

Table 6: Identification of best ANN architecture during the training process of residual soil slope data.

Network name	Training performed	Test performed	Validation performed	Training error	Test error	Validation error	Training algorithm	Error function	Hidden activation	Output activation
MLP 6-6-4	0.983	0.945	0.934	0.055	0.233	0.199	BFGS 31	SOS	Tanh	Exponential
MLP 6-9-4	0.976	0.949	0.913	0.076	0.215	0.226	BFGS 71	SOS	Logistic	Sine
MLP 6-2-4	0.884	0.901	0.886	0.360	0.404	0.305	BFGS 18	SOS	Exponential	Exponential
MLP 6-8-4	0.931	0.954	0.914	0.218	0.190	0.231	BFGS 30	SOS	Logistic	Identity
MLP 6-3-4	**0.977**	**0.966**	**0.915**	**0.073**	**0.145**	**0.223**	**BFGS 52**	**SOS**	**Logistic**	**Tanh**
MLP 6-14-4	0.893	0.910	0.881	0.333	0.369	0.330	BFGS 9	SOS	Identity	Exponential
MLP 6-8-4	0.954	0.953	0.905	0.147	0.209	0.246	BFGS 30	SOS	Logistic	Identity
MLP 6-3-4	0.965	0.938	0.902	0.112	0.260	0.170	BFGS 27	SOS	Tanh	Tanh
MLP 6-6-4	0.890	0.903	0.880	0.346	0.405	0.341	BFGS 17	SOS	Exponential	Exponential
MLP 6-8-4	0.967	0.940	0.895	0.106	0.257	0.275	BFGS 34	SOS	Tanh	Tanh
MLP 6-7-4	0.843	0.934	0.868	0.481	0.269	0.353	BFGS 3	SOS	Sine	Exponential
MLP 6-7-4	0.916	0.929	0.879	0.269	0.304	0.331	BFGS 33	SOS	Sine	Exponential
MLP 6-7-4	0.914	0.876	0.849	0.021	0.165	0.380	BFGS 76	SOS	Tanh	Exponential
MLP 6-5-4	0.886	0.912	0.885	0.359	0.363	0.315	BFGS 16	SOS	Exponential	Exponential
MLP 6-10-4	0.947	0.946	0.919	0.171	0.233	0.214	BFGS 31	SOS	Exponential	Sine

The bold values represent the best network architecture.

denote variables and rows denote instances. The total number of instances is 1200. The number of training instances is 720 (60%), the number of selection instances is 240 (20%), the number of testing instances is 240 (20%), and the number of unused instances is 0 (0%). If the data are very irregularly distributed, the model will probably become inferior quality. Table 7 lists the number of variables and their type. Table 8 lists the minimum, maximum, mean, and standard deviation of all the variables in the data set.

The most suitable neural network architecture was deduced by training, testing, and validating different combinations of hidden layers and associated neurons. A single hidden layer having a range of 2–15 neurons has been opted to train the neural network model. The number of neurons

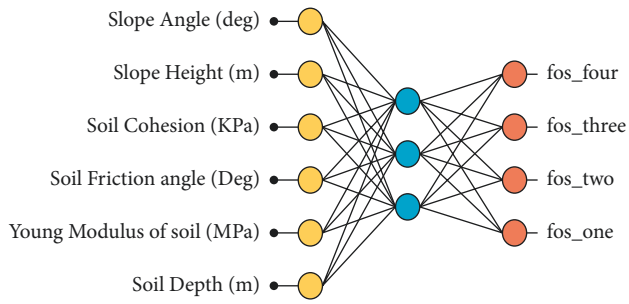

Figure 3: Neural network architecture for input and output in the case of the residual soil slope model.

Table 7: Variable table for rock slope.

Sr. no.	Name	Use
1	Slope angle (deg)	Input
2	Slope height (m)	Input
3	Width (m)	Input
4	Joint one	Input
5	Joint two	Input
6	FOS	Target

Table 8: Data statistics for prediction of rock slope stability.

Sr. no.	Rock slope parameter	Minimum	Maximum	Mean	Deviation
1	Slope angle (deg)	45	75	60	12.2526
2	Slope height (m)	100	500	300	141.48
3	Width (m)	2	10	6	2.82961
4	Joint one	1	4	2.5	1.1185
5	Joint two	1	4	2.5	1.1185
6	FOS	0.952	19.856	4.36915	3.21097

in the rest two layers, that is, the input layer and output layer, are constrained to the number of input variables and output variables, respectively [31]. The normalising of the input data was performed and the training process is initiated by randomly varying the number of neurons and their associated weights. The network with 5-10-1 architecture (five neurons in the input layer, ten neurons in a single hidden layer, and one neuron in the output layer) is selected based on maximum training performance and minimum training error for the developed ANN model after simulation of various network combinations (Table 9). The selected ANN model has a learning rate and momentum of 0.96 and 0.011, respectively, and its architecture is shown in Figure 4.

4.3. Efficiency of the Developed ANN Models. Several performance indices, as discussed in detail by Ray et al. [21] and Karir et al. [28], were used to measure the efficiency of the developed ANN models. The coefficient of determination (R^2) between the target and predicted values indicates a good prediction performance of the developed models. The RMSE and variance account for (VAF) were computed for studying the performance and the prediction capacity of the developed predictive models. Various performance indices obtained from the developed ANN1 model are presented in Table 10 and Figure 5.

5. Android Application

The developed app has two modules: one is residual soil classification, and the other is rock slope failure prediction using an artificial neural network. The neural network simulation has been done using neuro software. The simulation has been exported into code, and an equation has been used in developing the android app. Simulation of ANN also takes time and memory depending upon model complexity. Therefore, the equation generated from ANN simulation to predict classification and factor of safety was used. Smartphones have turned popular for the research for mobile applications because of their enhanced performance. This mobile application will be developed to facilitate the professionals to get a quick understanding of residual soil and rock slope behaviour to ascertain the potentially dangerous slopes. The smart miner app predicts the risk of slope failure for residual soil and rock, the factor of safety of rock slope, and the classification of residual soil (https://play.google.com/store/apps/details?id=com.maheshpaliwal.smartmineapp).

5.1. Debugging the Android Application. The android application offers dedicated tools to debug the app in Android Studio (IDE). There are two ways an Android app will be

Table 9: Identification of best ANN architecture during the training process of rock slope data.

Network name	Training performed	Test performed	Validation performed	Training error	Test error	Validation error	Training algorithm	Error function	Hidden activation	Output activation
MLP 5-6-1	0.983	0.945	0.934	0.055	0.233	0.199	BFGS 31	SOS	Tanh	Exponential
MLP 5-9-1	0.976	0.949	0.913	0.076	0.215	0.226	BFGS 71	SOS	Logistic	Sine
MLP 5-2-1	0.884	0.901	0.886	0.360	0.404	0.305	BFGS 18	SOS	Exponential	Exponential
MLP 5-8-1	0.931	0.954	0.914	0.218	0.190	0.231	BFGS 30	SOS	Logistic	Identity
MLP 5-10-1	**0.977**	**0.966**	**0.915**	**0.073**	**0.145**	**0.223**	**BFGS 52**	**SOS**	**Logistic**	**Tanh**
MLP 5-14-1	0.893	0.910	0.881	0.333	0.369	0.330	BFGS 9	SOS	Identity	Exponential
MLP 5-8-1	0.954	0.953	0.905	0.147	0.209	0.246	BFGS 30	SOS	Logistic	Identity
MLP 5-3-1	0.965	0.938	0.902	0.112	0.260	0.170	BFGS 27	SOS	Tanh	Tanh
MLP 5-6-1	0.890	0.903	0.880	0.346	0.405	0.341	BFGS 17	SOS	Exponential	Exponential
MLP 5-8-1	0.967	0.940	0.895	0.106	0.257	0.275	BFGS 34	SOS	Tanh	Tanh
MLP 5-7-1	0.843	0.934	0.868	0.481	0.269	0.353	BFGS 3	SOS	Sine	Exponential
MLP 5-7-1	0.916	0.929	0.879	0.269	0.304	0.331	BFGS 33	SOS	Sine	Exponential
MLP 5-7-1	0.914	0.876	0.849	0.021	0.165	0.380	BFGS 76	SOS	Tanh	Exponential
MLP 5-5-1	0.886	0.912	0.885	0.359	0.363	0.315	BFGS 16	SOS	Exponential	Exponential
MLP 5-10-1	0.947	0.946	0.919	0.171	0.233	0.214	BFGS 31	SOS	Exponential	Sine

The bold values represent the best network architecture.

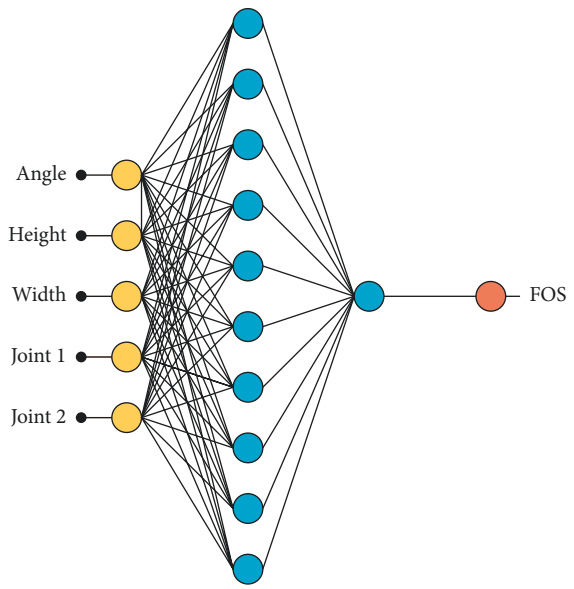

Figure 4: Neural network architecture for input and output in the case of the rock slope model.

Table 10: Performance indices of the developed ANN models.

Model	Data	R^2 (%)	RMSE	VAF (%)	Learning rate
ANN soil slope (MLP 6-3-4)	Training set	95.09	0.000403	98.74	0.91
	Testing set	92.95	0.00143	94.52	0.89
	Validating set	88.25	0.00217	93.30	0.85
ANN rock slope (MLP 5-10-1)	Training set	99.28	0.00014	99.22	0.96
	Testing set	98.96	0.00116	98.47	0.93
	Validating set	98.28	0.00184	97.26	0.92

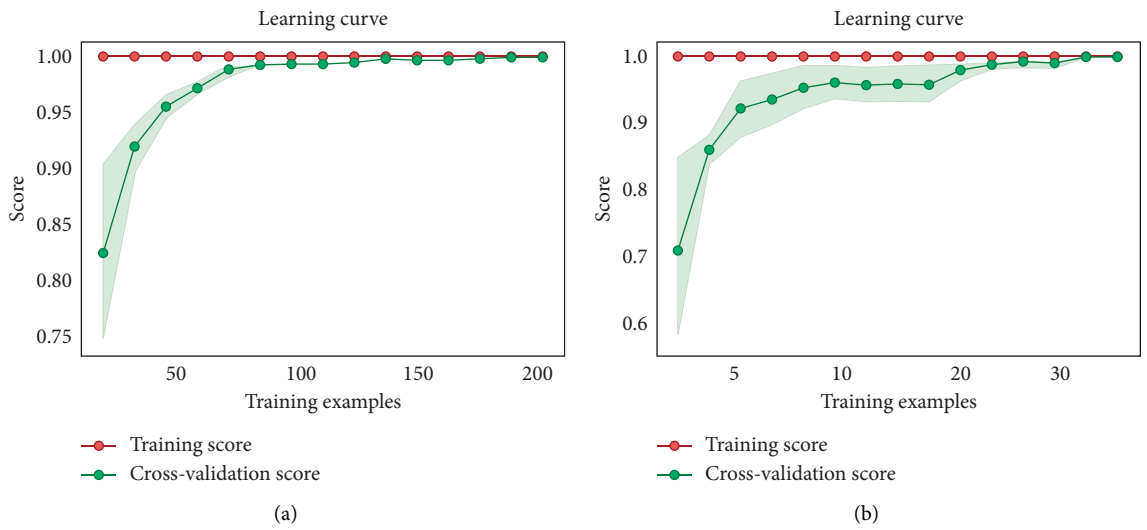

Figure 5: Leaning rate curve for the developed ANN model (a) rock slope and (b) residual soil slope.

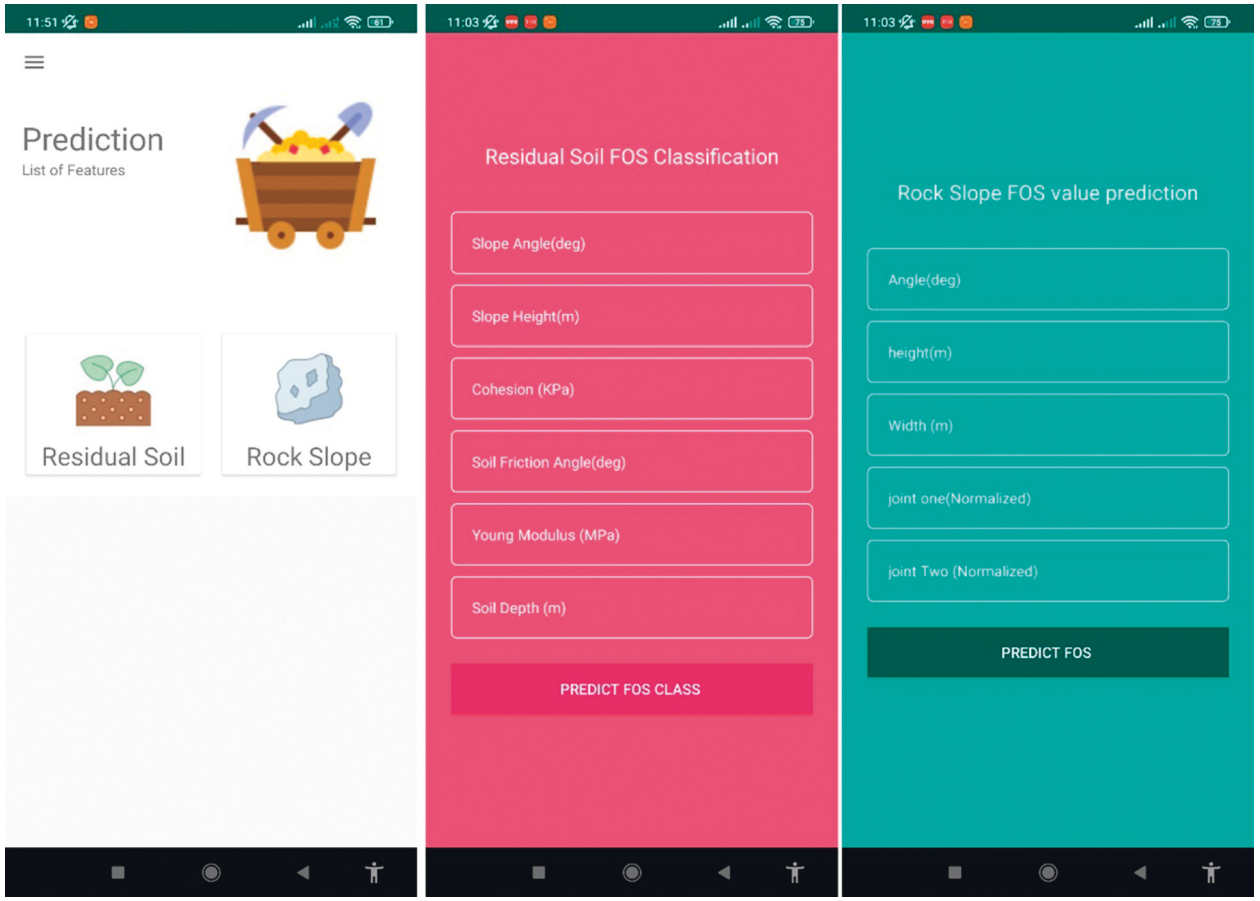

Figure 6: Layout of android app for prediction of classification and FOS.

debugged: first is the android simulator on the IDE itself and then the second is by testing the app on an actual Android smartphone. In this case, debugging the apps will be done in both ways and will them make stable and as reliable as possible.

5.2. Overview and Design of GUI. The app is built user friendly with a very basic GUI (Figure 6). The sample results are compared with various situations, and a very nice accord is achieved amongst them. The app helps the professionals to get a quick idea about residual soil and rock slope behaviour in order to identify the potential hazardous slopes.

5.3. Analysis of Residual Soil Classification for Safety Class. The inputs are slope angle, slope height, shear strength of residual soil, Young's modulus, and soil depth. The first step is that all parameter is scaled-down, and then y_1, y_2, and y_3 are calculated using the equation. The output is the probability of failure for all classes, that is, very low, low, medium, and high, is determined using the below-mentioned equation. The risk was predicted using the if-else rule and displayed in GUI using the Android application:

$$\begin{aligned}
\text{Scaled Angle (SA)} &= \frac{\text{Angle Degree} - 37.5}{16.7915},\\
\text{Scaled Height (SH)} &= \frac{2 \times (\text{Height} - 50)}{(500\text{–}50) - 1},\\
\text{Scaled Soil Cohesion (SSC)} &= \frac{2 \times (\text{Soil Cohesion} - 18)}{(20 - 18) - 1},\\
\text{Scaled Soil Friction Angle (SSFA)} &= \frac{2 \times (\text{Soil Frcition Angle} - 13.05)}{(50.84 - 13.05) - 1},\\
\text{Scaled Yound Modulus (SYM)} &= \frac{2\times}{(122.55\text{–}17.06)\text{–}1},\\
\text{Scaled Soil Depth (SSD)} &= \frac{\text{Soil Depth}}{4.61038}.
\end{aligned} \tag{1}$$

The generated parametric equations are as follows:

$$\begin{aligned}
Y_1 &= \text{SA} \times (-1.347) + \text{SH} \times (-0.3856) + \text{SSC} \times 0.1664 + \text{SSFA} \times (-0.6477) + \text{SYM} \times (-0.5756) + \text{SSD} \times (-14.2867) + 3.64855,\\
Y_2 &= \text{SA} \times (-11.119) + \text{SH} \times 0.0007 + \text{SSC} \times (-0.0094) + \text{SSFA} \times 0.03931\\
&\quad + \text{SYM} \times 0.03812 + \text{SSD} \times (-0.5750) - 5.29017,\\
Y_3 &= \text{SA} \times 11.558 + \text{SH} \times 0.1386 + \text{SSC} \times (-0.0789) + \text{SSFA} \times 0.0526\\
&\quad + \text{SYM} \times (-0.03475) + \text{SSD} \times 3.4199 - 7.22444.
\end{aligned} \tag{2}$$

The final output equations are as follows:

$$\begin{aligned}
\text{FOS one} &= \log(-4.88647 - 13.5303 \times \text{y_1} - 3.90927 \times \text{y_2} + 9.39114 \times \text{y_3}),\\
\text{FOS two} &= \log(5.09632 - 6.69187 \times y_1 - 21.403 \times y_2 - 9.24631 \times y_3),\\
\text{FOS three} &= \log(1.26147 - 5.43572 \times y_1 - 3.53762 \times y_2 - 15.1183 \times y_3),\\
\text{FOS four} &= \log(-5.10472 + 11.9405 \times y_1 + 8.98969 \times y_2 - 8.36946 \times y_3).
\end{aligned} \tag{3}$$

5.4. Analysis of Stability of Rock Slope. The inputs are slope angle, slope height, weathered layer thickness, joint one, and joint two. The first step is that all parameter is scaled-down, and then y_1 to y_10 are calculated using the equation generated. The final dependent variable is calculated using the tanh function and the set of generated equations. Equation 1 has been used to calculate the factor of safety of rock slope. The factor of safety is displayed in GUI using the Android application:

$$\begin{aligned}
\text{Scaled Angle (SA)} &= \frac{2 \times (\text{Angle} - 45)}{(75 - 45) - 1}, \\
\text{Scaled Height (SH)} &= \frac{\text{Height} - 300}{141.48}, \\
\text{Scaled Width (SW)} &= \frac{\text{Width} - 6}{2.82961}, \\
\text{Scaled Joint 1 } (\text{SJ}_1) &= \frac{\text{Joint 1} - 2.5}{1.1185}, \\
\text{Scaled Joint 2 } (\text{SJ}_2) &= \frac{\text{Joint 2} - 2.5}{1.1185}.
\end{aligned} \tag{4}$$

The generated parametric equations are as follows:

$$\begin{aligned}
y_1 &= \text{SA} \times (-0.0299) + \text{SH} \times 0.0052 + \text{SW} \times 0.7234 \\
&\quad + \text{SJ}_1 \times (-0.0178) + \text{SJ}_2 \times (-0.0613) + 1.4730, \\
y_2 &= \text{SA} \times 0.7511 + \text{SH} \times (-0.0725) + \text{SW} \times 0.2719 \\
&\quad + \text{SJ}_1 \times 0.1946 + \text{SJ}_2 \times 0.3301 - 0.0513, \\
y_3 &= \text{SA} \times 1.9950 + \text{SH} \times 0.0088 + \text{SW} \times 0.1001 \\
&\quad + \text{SJ}_1 \times 0.0180 + \text{SJ}_2 \times 1.0704 + 1.8012, \\
y_4 &= \text{SA} \times 0.8161 + \text{SH} \times (-0.2945) + \text{SW} \times 0.0104 \\
&\quad + \text{SJ}_1 \times 0.8764 + \text{SJ}_2 \times (-1.1940) + 0.5068, \\
y_5 &= \text{SA} \times (-0.6566) + \text{SH} \times 0.1560 + \text{SW} \times 0.2316 \\
&\quad + \text{SJ}_1 \times (-0.2772) + \text{SJ}_2 \times (-0.4959) - 0.9843, \\
y_6 &= \text{SA} \times 0.6504 + \text{SH} \times (-0.3412) + \text{SW} \times 1.2101 \\
&\quad + \text{SJ}_1 \times 0.5729 + \text{SJ}_2 \times (-0.0108) + 0.6504, \\
y_7 &= \text{SA} \times (-0.8111) + \text{SH} \times 0.2632 + \text{SW} \times (-0.2796) \\
&\quad + \text{SJ}_1 \times 0.9308 + \text{SJ}_2 \times (-0.1901) - 1.9974, \\
y_8 &= \text{SA} \times (-0.0666) + \text{SH} \times (-0.1778) + \text{SW} \times (-0.7677) \\
&\quad + \text{SJ}_1 \times 0.4441 + \text{SJ}_2 \times (-0.0806) - 0.8139, \\
y_9 &= \text{SA} \times 0.6675 + \text{SH} \times (-0.8984) + \text{SW} \times (-0.8047) \\
&\quad + \text{SJ}_1 \times 0.1252 + \text{SJ}_2 \times (-0.0890) - 0.3682, \\
y_{10} &= \text{SA} \times 1.1990 + \text{SH} \times 0.1535 + \text{SW} \times (-0.2116) \\
&\quad + \text{SJ}_1 \times (-1.4960) + \text{SJ}_2 \times 0.3974 + 1.4552.
\end{aligned} \tag{5}$$

Table 11: Factor of safety from modelling and Android app for residual soil classification.

Sr. no.	Slope angle (deg)	Slope height (m)	Soil cohesion (kPa)	Friction angle (deg)	Young's modulus of soil (MPa)	Soil depth (m)	Class from modelling	Chance of failure from app
1	60	200	18.5	35	86	2	High	High
2	45	250	20.0	39	98	5	High	High
3	45	300	19.5	15	62	2	Medium	Medium
4	60	100	19.0	39	77	2	High	High
5	30	100	20.0	15	65	9	Medium	Medium
6	45	450	19.0	21	91	1	Medium	Medium
7	30	150	19.0	37	97	12	Medium	Medium
8	15	300	20.0	18	49	9	Very low	Very low
9	15	200	19.5	49	91	15	Very low	Very low
10	30	500	18.5	47	46	3	Low	Low

Table 12: Factor of safety from modelling and Android app for rock slope stability.

Sr. no.	Slope angle (deg)	Slope height (m)	Width (m)	Joint one (deg)	Joint two (deg)	FOS from modelling	FOS from app
1	45	200	8	−65	−50	2.12	2.08
2	45	300	8	−65	−50	1.81	1.87
3	45	100	2	−45	10	7.11	7.26
4	60	400	6	−65	−10	1.49	1.59
5	75	100	6	−25	−30	2.68	2.53
6	75	200	10	−65	−10	1.30	1.43
7	75	500	8	−65	10	1.27	1.23
8	60	500	8	−65	−10	1.16	1.26
9	60	200	6	−65	−10	1.568	1.73
10	60	100	2	−5	−30	8.40	8.45

The final generated parametric equations are as follows:-

$$
\begin{aligned}
Y_1 &= y_1 \times 0.984 + y_2 \times (-0.882) + y_3 \times 0.421 + y_4 \times (-0.993) + y_5 \times (-0.871) + y_6 \times 0.422 + y_7 \times (-0.528) + y_8 \times 0.012 \\
&\quad + y_9 \times (-0.116) + y_{10} \times (-0.004) - 0.309, \\
Y_2 &= y_1 \times 0.065 + y_2 \times 0.234 + y_3 \times 0.268 + y_4 \times 0.669 + y_5 \times (-0.646) + y_6 \times (-0.110) + y_7 \times (-0.133) + y_8 \times (-1.282) \\
&\quad + y_9 \times 0.639 + y_{10} \times (-0.602) + 1.554, \\
Y_3 &= y_1 \times 0.040 + y_2 \times 0.281 + y_3 \times 0.231 + y_4 \times (-0.076) + y_5 \times (-0.065) + y_6 \times (-0.027) + y_7 \times (-0.137) + y_8 \times (-0.126) \\
&\quad + y_9 \times 0.141 + y_{10} \times (-0.311) - 0.204, \\
Y_4 &= y_1 \times 1.121 + y_2 \times 0.807 + y_3 \times 0.784 + y_4 \times 0.91 + y_5 \times 0.151 + y_6 \times (-1.382) + y_7 \times (-1.403) + y_8 \times (-0.751) + y_9 \\
&\quad \times (-0.897) + y_{10} \times (-1.482) + 1.138, \\
Y_5 &= y_1 \times (-0.353) + y_2 \times (-0.403) + y_3 \times 0.170 + y_4 \times (-0.645) + y_5 \times 0.748 + y_6 \times 0.371 + y_7 \times (-0.314) + y_8 \times 0.288 \\
&\quad - y_9 \times (-0.299) + y_{10} \times 0.131 + 0.877.
\end{aligned} \tag{6}
$$

The final output equations are as follows:

$$
\begin{aligned}
\text{Scaled FOS} &= 0.387946 \times Y_1 + 2.45703 \times Y_2 - 1.47291 \times Y_3 - 1.74675 \times Y_4 \\
&\quad - 0.457422 \times Y_5 - 0.329065 \\
\text{FOS} &= (0.5 \times (\text{scaled\_FOS} + 1.0) \times (19.856 - 0.952) + 0.952).
\end{aligned} \tag{7}
$$

5.5. Prediction of Stability Class and Factor of Safety Using Android Application. After verifying and debugging, the developed app is tested on three real android mobiles; Samsung (model: SM-N750), Asus (model: ASUS T_00J), and Xiaomi (model: Mi Note 8 Pro); it is concluded here that a good agreement is achieved between computed results and their reference counterparts for all seven cases associated with the example. The values for a particular case are listed in Tables 11 and 12. A particular case is presented in these tables. The app results are in normalised form by default, which can be converted before use. The app has two modules: one is residual soil classification and the other is rock slope failure prediction using an artificial neural network. Table 11 lists the prediction classification of residual soil using the ANN algorithm and android app. Table 12 lists the prediction of FOS of rock slope using the ANN algorithm and android app.

6. Conclusions

There are various problems associated with calculating the factor of safety of the hills in the Himalayan region. Various tests are to be performed, which are very time consuming and expensive. As by nature, the slopes are not uniform. There can be a sudden change in the geomaterial (soil to rock and vice versa) within a few hundred meters. Thus, carrying out conventional geotechnical investigations over a stretch having several rocks and soil slope is very cumbersome. An effort has been made to quickly identify the stability of both the rock slope and residual soil slope. Numerical simulation results from previous studies on residual soil and rock slope were used to develop the ANN models. Various performance indices were used to highlight the high efficiency of the developed ANN models. The developed ANN models were further used to develop a mobile application for slope stability assessment.

The proposed software is user friendly and economical (virtually no cost) and has been constructed on an artificial neural network application intended in place of microstrip antenna applications. The performance viability of the developed mobile application has been verified using the virtual android platform in the IDE itself and then utilising various real-world android mobiles possessing unique chipset configurations ranging from higher performance to lower performance. All the mobile devices performed quite positively, providing the same desired results for all use cases. Thus, the proposed solution delivers a roadmap for the development of an android app utilising artificial neural networks due to which the proposed methodology is reasonably faster and has a lower manufacturing cost.

Data Availability

Data available on request

Conflicts of Interest

The authors declare that they have no conflicts of interest.

References

[1] A. Ray, A. K. Bharati, R. Rai, and T. Singh, "Landslide occurrences in Himalayan residual soil: a review," *Himalayan Geology*, vol. 42, pp. 189–204, 2021.

[2] O. Hungr, S. Leroueil, and L. Picarelli, "The Varnes classification of landslide types, an update," *Landslides*, vol. 11, no. 2, pp. 167–194, 2014.

[3] G. L. S. Babu and M. Mukesh, "Risk analysis of landslides–A case study," *Geotechnical & Geological Engineering*, vol. 21, no. 2, pp. 113–127, 2003.

[4] H. Ballabh, S. Pillay, G. C. S. Negi, and K. Pillay, "Relationship between selected physiographic features and landslide occurrence around four hydropower projects in Bhagirathi valley of Uttarakhand, Western Himalaya, India," *International Journal of Geosciences*, vol. 04, no. 10, pp. 1088–1099, 2014.

[5] Rahul, M. Khandelwal, R. Rai, and B. K. Shrivastva, "Evaluation of dump slope stability of a coal mine using artificial neural network," *Geomechanics and Geophysics for Geo-Energy and Geo-Resources*, vol. 1, no. 3-4, pp. 69–77, 2015.

[6] P. Aleotti and R. Chowdhury, "Landslide hazard assessment: summary review and new perspectives," *Bulletin of Engineering Geology and the Environment*, vol. 58, no. 1, pp. 21–44, 1999.

[7] R. Bhambri, M. Mehta, S. Singh, R. Jayangondaperumal, A. K. Gupta, and P. Srivastava, "Landslide inventory and damage assessment in the bhagirathi valley, Uttarakhand, during june 2013 flood," *Himalayan Geology*, vol. 38, pp. 193–224, 2017.

[8] D. Petley, "Global patterns of loss of life from landslides," *Geology*, vol. 40, no. 10, pp. 927–930, 2012.

[9] R. L. Schuster and R. W. Fleming, "Economic losses and fatalities due to landslides," *Environmental and Engineering Geoscience*, vol. xxiii, no. 1, pp. 11–28, 1986.

[10] F. C. Dai, C. F. Lee, and Y. Y. Ngai, "Landslide risk assessment and management: an overview," *Engineering Geology*, vol. 64, no. 1, pp. 65–87, 2002.

[11] R. Bhasin, E. Grimstad, J. O. Larsen et al., "Landslide hazards and mitigation measures at Gangtok, Sikkim Himalaya," *Engineering Geology*, vol. 64, no. 4, pp. 351–368, 2002.

[12] D. Chatterjee and A. Murali Krishna, "Effect of slope angle on the stability of a slope under rainfall infiltration," *Indian Geotechnical Journal*, vol. 49, no. 6, pp. 708–717, 2019.

[13] M. Ghimire, "Landslide occurrence and its relation with terrain factors in the Siwalik Hills, Nepal: case study of susceptibility assessment in three basins," *Natural Hazards*, vol. 56, no. 1, pp. 299–320, 2011.

[14] A. Clerici, S. Perego, C. Tellini, and P. Vescovi, "A procedure for landslide susceptibility zonation by the conditional analysis method," *Geomorphology*, vol. 48, no. 4, pp. 349–364, 2002.

[15] D. Kanungo, M. Arora, S. Sarkar, and R. Gupta, "Landslide susceptibility zonation (LSZ) mapping–A review," *Journal of South Asia Disaster Studies*, vol. 2, 2009.

[16] B. M. Marrapu and R. S. Jakka, "Landslide hazard zonation methods: a critical Review," *International Journal of Civil Engineering Research*, vol. 5, pp. 215–220, 2014.

[17] S. Sarkar, D. P. Kanungo, and G. S. Mehrotra, "Landslide hazard zonation: a case study in garhwal himalaya, India," *Mountain Research and Development*, vol. 15, no. 4, pp. 301–309, 1995.

[18] A. Ray, R. E. S. C. Kumar, A. K. Bharati, R. Rai, and T. N. Singh, "Hazard chart for identification of potential

landslide due to the presence of residual soil in the Himalayas," *Indian Geotechnical Journal*, vol. 50, no. 4, pp. 604–619, 2020a.

[19] A. Ray, R. Rai, and T. N. Singh, "The effect of discontinuity orientation and thickness of the weathered layer on the stability of lesser himalayan rock slope," *Journal of the Geological Society of India*, vol. 98, no. 2, pp. 260–270, 2022.

[20] S. Agatonovic-Kustrin and R. Beresford, "Basic concepts of artificial neural network (ANN) modeling and its application in pharmaceutical research," *Journal of Pharmaceutical and Biomedical Analysis*, vol. 22, no. 5, pp. 717–727, 2000.

[21] A. Ray, V. Kumar, A. Kumar, R. Rai, M. Khandelwal, and T. N. Singh, "Stability prediction of Himalayan residual soil slope using artificial neural network," *Natural Hazards*, vol. 103, no. 3, pp. 3523–3540, 2020b.

[22] S. Kumar and P. K. Basudhar, "A neural network model for slope stability computations," *Géotechnique Letters*, vol. 8, no. 2, pp. 149–154, 2018.

[23] B. Kalantar, B. Pradhan, S. A. Naghibi, A. Motevalli, and S. Mansor, "Assessment of the effects of training data selection on the landslide susceptibility mapping: a comparison between support vector machine (SVM), logistic regression (LR) and artificial neural networks (ANN)," *Geomatics, Natural Hazards and Risk*, vol. 9, no. 1, pp. 49–69, 2018.

[24] M. Khajehzadeh, M. R. Taha, S. Keawsawasvong, H. Mirzaei, and M. Jebeli, "An effective artificial intelligence approach for slope stability evaluation," *IEEE Access*, vol. 10, 2022.

[25] W. Gao, M. Raftari, A. S. A. Rashid, M. A. Mu'azu, and W. A. W. Jusoh, "A predictive model based on an optimized ANN combined with ICA for predicting the stability of slopes," *Engineering with Computers*, vol. 36, no. 1, pp. 325–344, 2020.

[26] S. E. Cho, "Probabilistic stability analyses of slopes using the ANN-based response surface," *Computers and Geotechnics*, vol. 36, no. 5, pp. 787–797, 2009.

[27] A. K. Verma, T. N. Singh, N. K. Chauhan, and K. Sarkar, "A hybrid FEM-ANN approach for slope instability prediction," *Journal of The Institution of Engineers (India): Series A*, vol. 97, no. 3, pp. 171–180, 2016.

[28] D. Karir, A. Ray, A. K. Bharati, U. Chaturvedi, R. Rai, and M. Khandelwal, "Stability prediction of a natural and man-made slope using various machine learning algorithms," *Transportation Geotechnics*, vol. 34, Article ID 100745, 2022.

[29] A. K. Bharati, A. Ray, M. Khandelwal, R. Rai, and A. Jaiswal, "Stability evaluation of dump slope using artificial neural network and multiple regression," *Engineering with Computers*, pp. 1–9, 2021.

[30] J. P. Bharti, P. Mishra, V. Sathishkumar, Y. Cho, and P. Samui, "Slope stability analysis using Rf, gbm, cart, bt and xgboost," *Geotechnical & Geological Engineering*, vol. 39, pp. 1–12, 2021.

[31] M. Ghiasi, N. Askarnejad, S. R. Dindarloo, and H. Shamsoddini, "Prediction of blast boulders in open pit mines via multiple regression and artificial neural networks," *International Journal of Mining Science and Technology*, vol. 26, no. 2, pp. 183–186, 2016.